

Supplementary Material

A) Detailed methodology

560 Adopting the approach of Tobin et al. (2016), we use near-surface wind speeds 10 meters above the ground. Assuming a power-law relationship for the vertical wind profile, the velocity at hub height H is obtained as

$$v_H = v_{10m} \cdot \left(\frac{H}{10} \right)^{\frac{1}{7}} \quad (9)$$

and we chose $H = 80m$.

565 The conversion of wind speeds into renewable generation is performed using a simple power curve

$$P(v_H) = P_0 \begin{cases} 0, & \text{if } v_H < v_i \text{ or } v_H > v_0 \\ \frac{v_H^3 - v_i^3}{v_R^3 - v_i^3}, & \text{if } v_i \leq v_H < v_R \\ 1, & \text{if } v_R \leq v_H < v_0 \end{cases} \quad (10)$$

where v_H denotes wind velocity at hub height and $v_i = 3.5$ m/s, $v_R = 12$ m/s, $v_0 = 25$ m/s denote the cut-in, rated and cut-out velocity of the wind turbine, respectively. We assume that every wind park has a capacity $P_0 = 0.1$ GW.

570 If the number of wind parks per grid cell $N_{\text{wind}}(x, y)$ is known, the renewable generation in a country with area A_i is given by

$$P_i(t) = \sum_{x, y \in A_i} N_{\text{wind}}(x, y) \cdot P(v_H(x, y, t)). \quad (11)$$

Note that we assume a stationary configuration of wind parks throughout every 20 year period. Moreover, we assume that each country generates as much energy from renewables as is needed in

575 a 20 year period ranging from t_{start} to t_{end}

$$\int_{t_{\text{start}}}^{t_{\text{end}}} P_i(t) dt = \int_{t_{\text{start}}}^{t_{\text{end}}} D_i(t) dt \quad (12)$$

Since all variables except from N_{wind} are used as input to the model, and hence are known, equations (11) and (12) can be used to determine N_{wind} . However, the solution is degenerate. In order to single out one solution, we adopt the strategy of Monforti et al. (2016) who distribute wind parks

580 randomly at those places where the temporal average of renewable generation P is above average.

Performing a Monte Carlo analysis for the deployment of wind parks, Monforti et al. found that the sensitivity of this partially random allocation procedure to changes in the actual configuration of N_{wind} is small.

Transmission

585 The imports/exports F_i of a country i (see Eq. (2)) depend on the incidence matrix

$$K_{i,l} = \begin{cases} 1, & \text{if line } l \text{ starts in country } i \\ -1 & \text{if line } l \text{ ends in country } i \\ 0 & \text{otherwise} \end{cases} \quad (13)$$

and the flows \hat{F}_l along a line l

$$F_i = - \sum_l K_{i,l} \hat{F}_l, \quad (14)$$

where the minus sign stems from the (arbitrary) choice that $F_i > 0$ means imports. The flow along a
590 line l is bound by

$$\alpha \cdot \text{NTC}_{l-} \leq \hat{F}_l \leq \alpha \cdot \text{NTC}_{l+}, \quad (15)$$

where α denotes grid expansion. The line limits $\text{NTC}_{l+} \geq 0$ and $\text{NTC}_{l-} \leq 0$ are direction dependent and the former refers to the line limit in the direction of line l as defined via the incidence matrix (13). Line limits are directional winter Net Transfer Capacities published by ENTSO-E for 2010/2011
595 (European Network of Transmission System Operators for Electricity, 2011).

Inclusion of PV generation

We use PV generation timeseries from Pfenninger and Staffell (2016) which is more complete than other open source datasets like Open Power System Data¹. The data set is bias corrected and validated at around 1000 locations. We favored to use the part of the dataset which is based on MERRA
600 over SARAH because the latter is lacking data in the first years.

We average over 30 years of data to compute a representative PV generation timeseris $PV_i(t)$ for every country i . Using a representative year is not an ideal approach since inter-year variations are artificially muted. However, the PV generation timeseries only exists for the historical period. If one was to combine PV generations from one year with wind generations from another, the result is
605 likely to be unrealistic because the corresponding state of the climate system belonging to either the PV or wind generation would be out of phase. We thus consider our approach to be the most suitable one in this assessment.

In order to incorporate PV generation into the model, we replace the original load $D_i(t)$ in Eq. (1) with the residual load after PV generation is subtracted as

¹ <http://www.open-power-system-data.org/>

$$610 \quad D_i(t) \rightarrow D_i(t) - \gamma \cdot PV_i(t), \quad (16)$$

where γ is chosen such that 29% of the overall generation is contributed by PV. This share has been found to be the European optimum in terms of minimizing backup needs in a similar setup (Rodriguez et al., 2014). The load $D_i(t)$ now represents the residual load which has to be satisfied by wind, im-/exports or dispatchable power plants. Results including PV are shown in Supplement

615 B.

Sensitivity to load timeseries

We repeat our analysis assuming constant loads

$$D_i(t) \rightarrow \langle \hat{D}_i(t) \rangle_t, \quad (17)$$

where $\hat{D}_i(t)$ denotes monthly load data from ENTSO-E and $\langle \cdot \rangle_t$ denotes the temporal average. The

620 goal of muting the time dependency of the load is to test for the influence of the load timeseries on our modelling outcomes. Results for constant loads are shown in Supplement C.

B) Energy results including PV

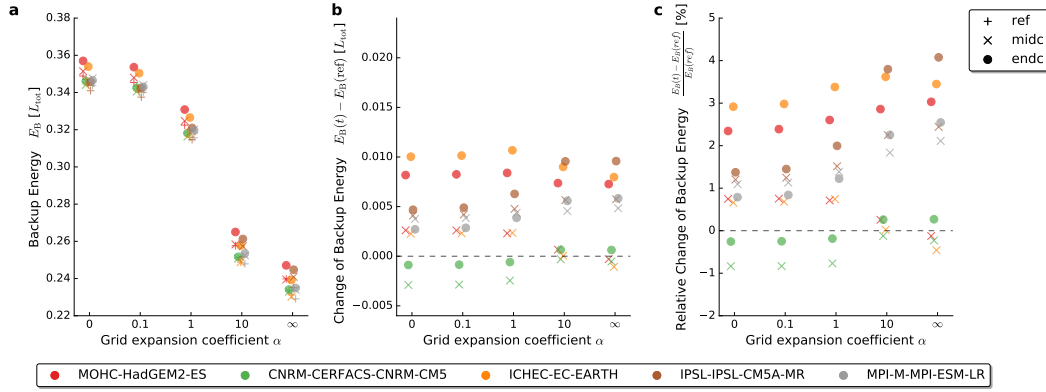


Figure 8. Same as Fig. 2, but including PV from Pfenninger and Staffell (2016).

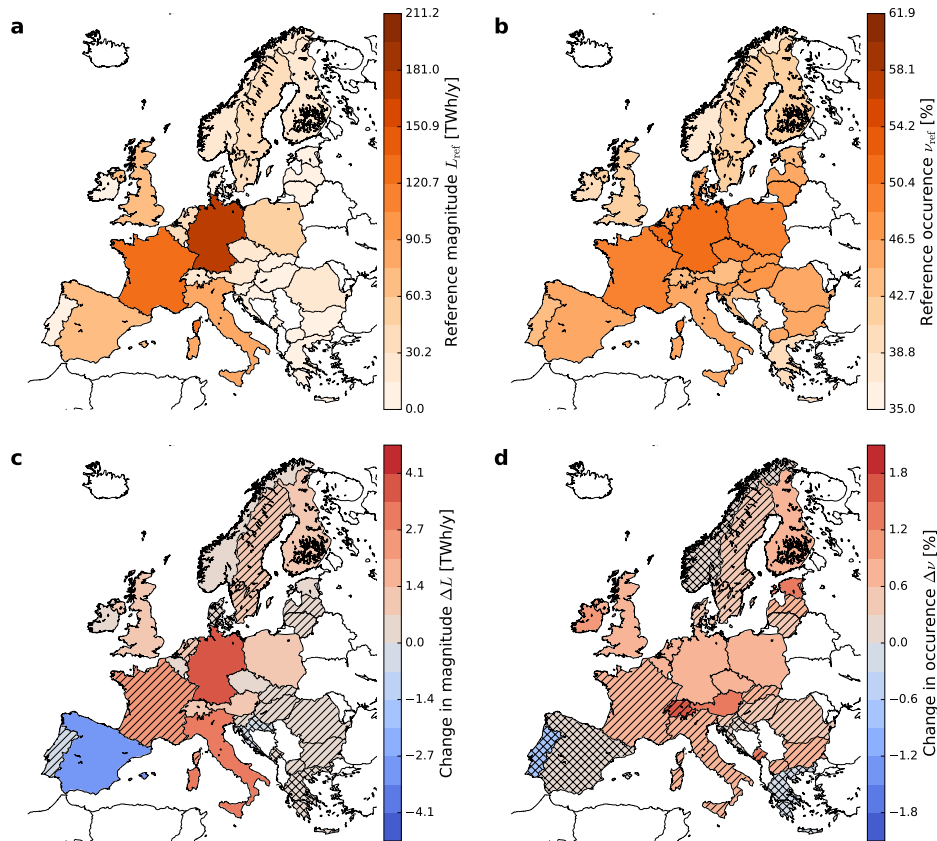


Figure 9. Same as Fig. 3 but including PV from Pfenninger and Staffell (2016).

C) Energy results assuming constant loads

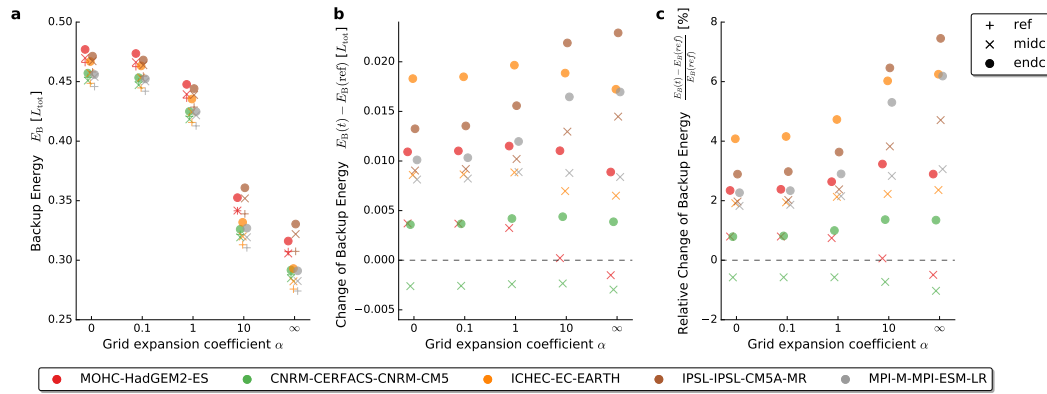


Figure 10. Same as Fig. 2, but with constant load.

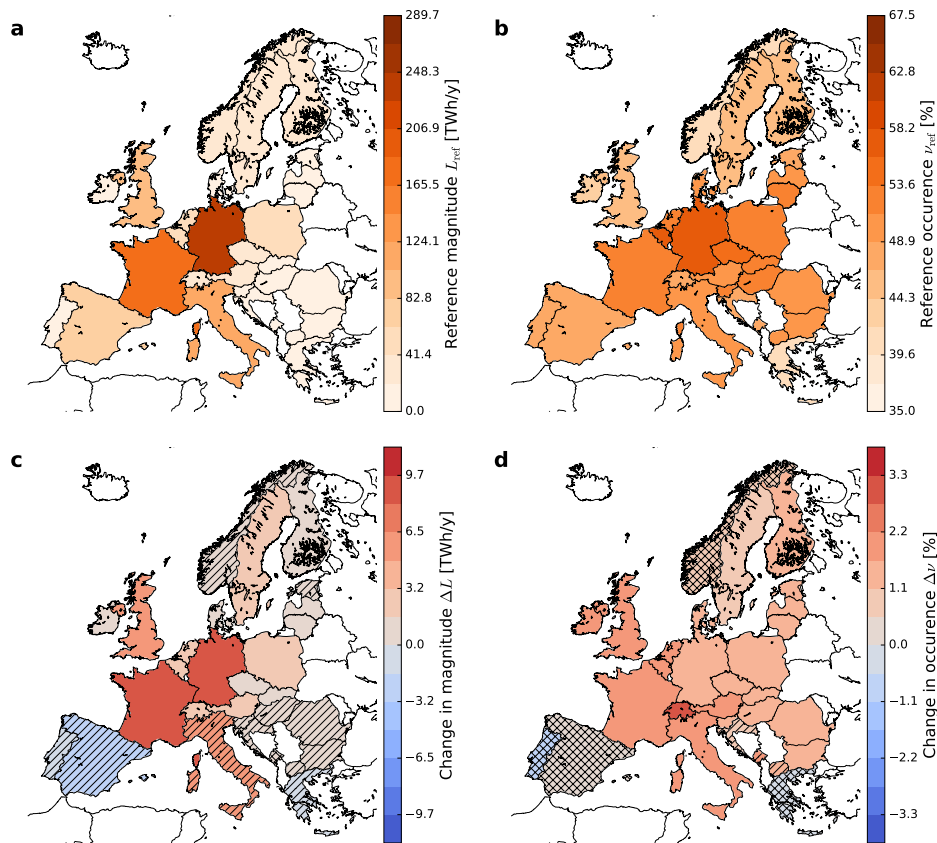


Figure 11. Same as Fig. 3 but assuming constant load.

D) Correlations by mid century

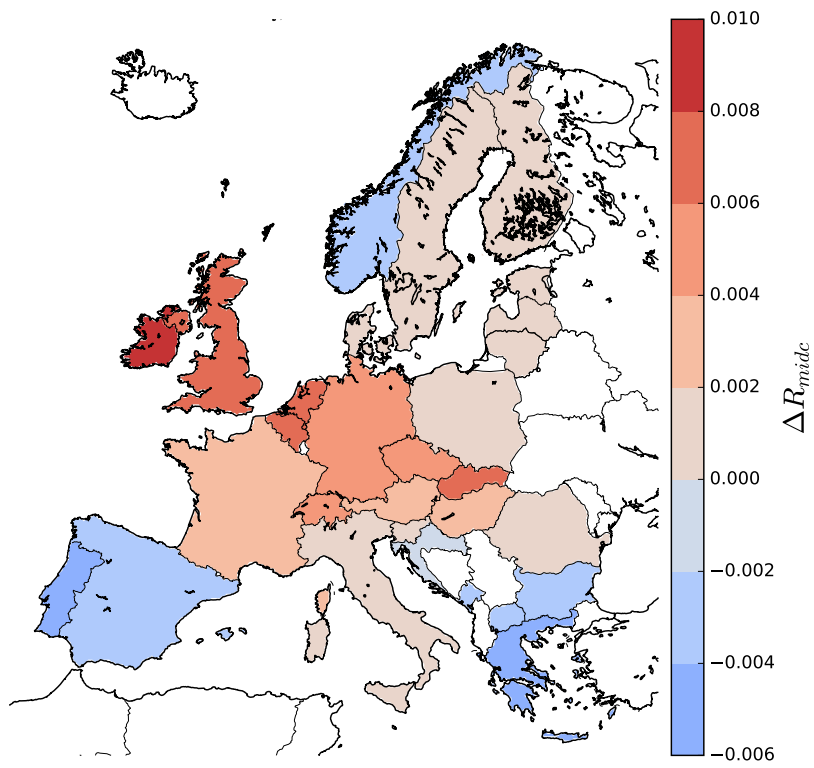


Figure 12. Same as Fig. 4 but for mid century.

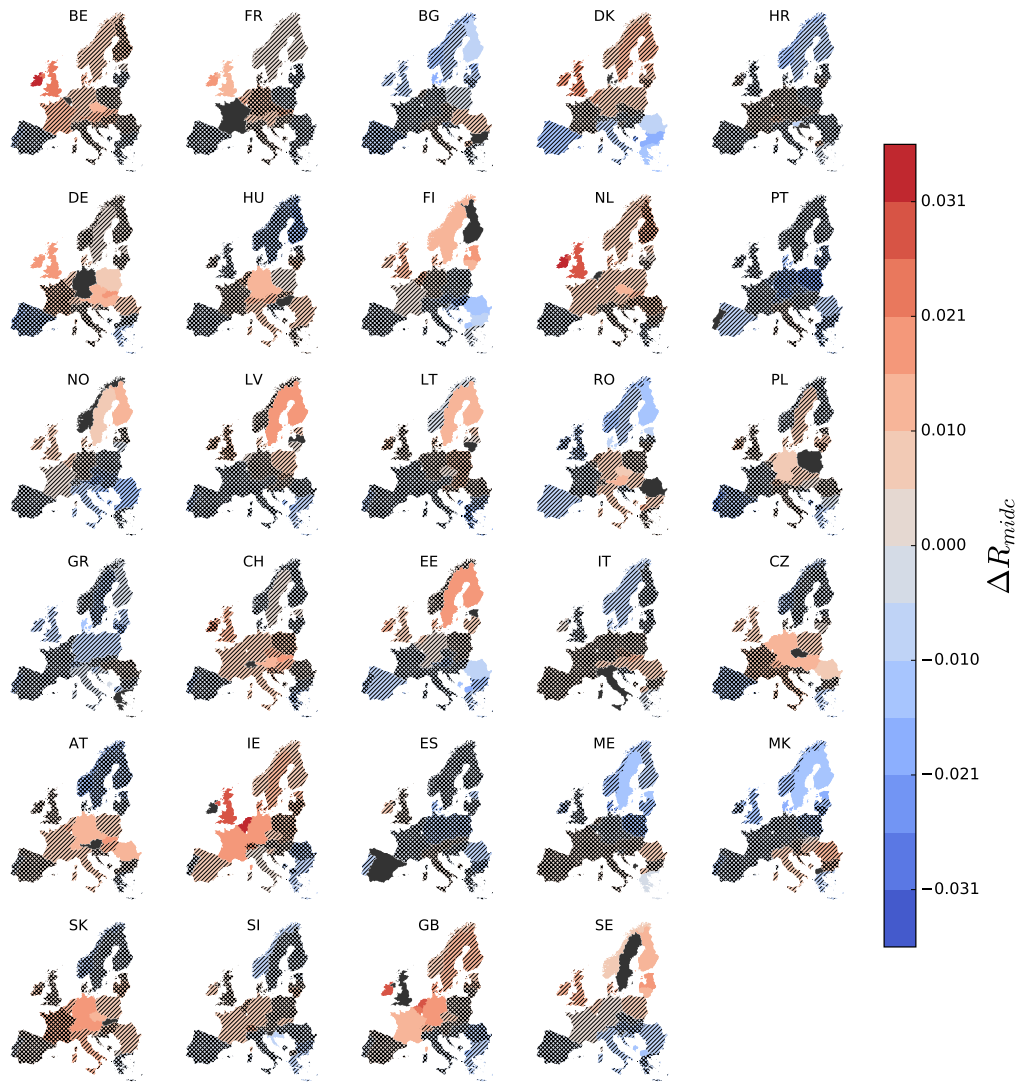


Figure 13. Same as Fig. 5 but for mid century.

625 E) Spatial homogeneity and CWTs

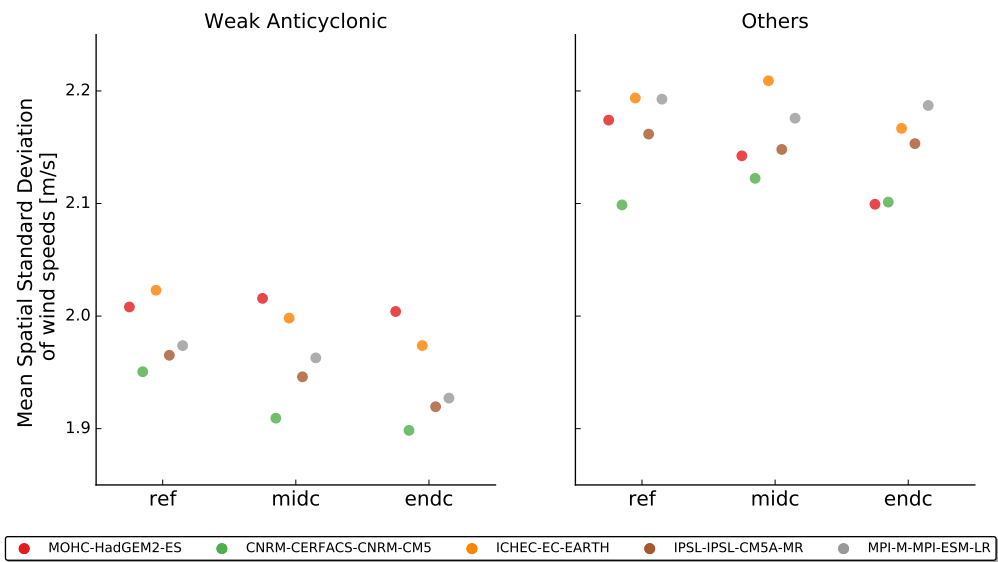


Figure 14. Mean spatial standard deviation of wind speeds over all 28 countries considered in the energy assessment. The standard deviation is calculated for each grid point separately. The weak anticyclonic CWT has a distinctly smaller spatial standard deviation than all other situations considered together. Hence, it is characterized by more homogeneous wind fields.